

## Rewritable Glycochips

L. G. Harris,<sup>‡</sup> W. C. E. Schofield,<sup>‡</sup> K. J. Doores,<sup>†</sup> B. G. Davis,<sup>†</sup> and  
J. P. S. Badyal<sup>\*†</sup>

*Department of Chemistry, Science Laboratories, Durham University,  
Durham DH1 3LE, U.K., and Department of Chemistry, University of Oxford, Chemistry  
Research Laboratory, Mansfield Road, Oxford OX1 3TA, U.K.*

Received February 19, 2009; E-mail: j.p.badyal@durham.ac.uk

**Abstract:** We describe microarraying of carbohydrates for protein screening using either disulfide bridge or Schiff base imine immobilization chemistries on plasmachemical deposited functional nanolayers. The commonly observed issue of nonspecific background binding of proteins is overcome by spotting carbohydrates through a protein-resistant overlayer yielding spatially localized interaction with a reactive functional underlayer.

### 1. Introduction

Carbohydrate–protein interactions mediate a whole host of biological mechanisms, including those responsible for viral infection,<sup>1,2</sup> cancer metastasis,<sup>3,4</sup> peptide conformation,<sup>5</sup> enzyme activity,<sup>6</sup> cell–cell recognition,<sup>7,8</sup> cell adhesion,<sup>9,10</sup> and cell development.<sup>11</sup> Methods commonly employed to probe these systems include electrospray ionization mass spectrometry,<sup>12</sup> fluorescence microscopy,<sup>13</sup> chromatography,<sup>14</sup> X-ray crystallography,<sup>15,16</sup> and NMR spectroscopy.<sup>17</sup> Although of great use, these techniques can be time-consuming, expensive, and sometimes difficult to interpret. A promising alternative approach is to screen molecular arrays of immobilized carbohydrates in a

similar fashion to DNA<sup>18–20</sup> and protein<sup>21–23</sup> chips. These effectively offer a high-throughput and low-cost solution to studying carbohydrate–protein interactions.

Generically several approaches have evolved for carbohydrate immobilization onto solid surfaces. These include thiol-terminated carbohydrate self-assembled monolayers (SAMs) on gold,<sup>24–26</sup> Diels–Alder coupling of carbohydrate–cyclopentadiene conjugated to thiol-terminated benzoquinone SAMs,<sup>27,28</sup> hydrophobic attachment of C<sub>13</sub>–C<sub>15</sub> saturated alkyl-terminated carbohydrates to polystyrene microtiter plates,<sup>29–32</sup> arraying onto nitrocellulose membranes,<sup>33</sup> electrostatic deposition of carbohydrates,<sup>34</sup> and covalent immobilization of modified carbohydrates directly onto functionalized glass slides<sup>35–42</sup> or silicon.<sup>43,44</sup> However, most of these methods suffer from drawbacks such as poor shelf life (e.g., SAMs<sup>24–28</sup> attributable to the low Au–S bond enthalpy triggering oxidation and desorption processes at

<sup>‡</sup> Durham University.

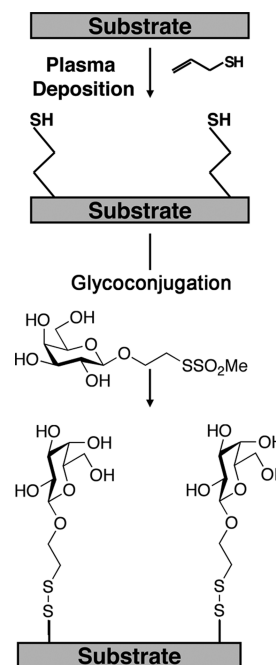
<sup>†</sup> University of Oxford.

- (1) Dwek, R. A. *Chem. Rev.* **1996**, *96*, 683.
- (2) Kitov, P. I.; Sadowska, J. M.; Mulvey, G.; Armstrong, G. D.; Ling, H.; Pannu, N. S.; Read, R. J.; Bundle, D. R. *Nature* **2000**, *403*, 669.
- (3) Joo, K. L.; Mao, S.; Sun, C.; Gao, C.; Blixt, O.; Arrues, S.; Hom, L. G.; Kaufmann, G. F.; Hofmann, T. Z.; Coyle, A. R.; Paulson, J.; Felding-Habermann, B.; Janda, K. D. *J. Am. Chem. Soc.* **2002**, *124*, 12439.
- (4) McCever, R. P. *Glycoconjugate J.* **1997**, *14*, 585.
- (5) Bosques, C. J.; Tschampel, S. M.; Woods, R. J.; Imperiali, B. *J. Am. Chem. Soc.* **2004**, *126*, 8421.
- (6) Major, L. L.; Wolucka, B. A.; Naismith, J. H. *J. Am. Chem. Soc.* **2005**, *127*, 18309.
- (7) Lis, H.; Sharon, N. *Chem. Rev.* **1998**, *98*, 637.
- (8) Flitsch, S. L.; Ulijn, R. V. *Nature* **2003**, *421*, 219.
- (9) Dove, A. *Nature* **2000**, *19*, 913.
- (10) Disney, M. D.; Zheng, J.; Swager, T. M.; Seeberger, P. H. *J. Am. Chem. Soc.* **2004**, *126*, 13343.
- (11) Bertozzi, C. R.; Kiessling, L. L. *Science* **2001**, *291*, 2357.
- (12) Sun, J.; Kitova, E. N.; Wang, W.; Klassen, J. S. *Anal. Chem.* **2006**, *78*, 3010.
- (13) Liao, J. H.; Chen, C. T.; Chou, H. C.; Cheng, C. C.; Chou, P. T.; Fang, J. M.; Slanina, Z.; Chow, T. J. *Org. Lett.* **2002**, *4*, 3107.
- (14) Striegler, A. M. *J. Am. Chem. Soc.* **2003**, *125*, 4146.
- (15) Olsen, L. R.; Dessen, A.; Gupta, D.; Sabesan, S.; Sacchettini, J. C.; Brewer, C. F. *Biochemistry* **1997**, *36*, 15073.
- (16) Vyas, N. K.; Meenakshi, N. V.; Chervenak, M. C.; Johnson, M. A.; Mario Pinto, B.; Bundle, D. R.; Quioccho, F. A. *Biochemistry* **2002**, *41*, 13575.
- (17) Haselhorst, T.; Weimar, T.; Peters, T. *J. Am. Chem. Soc.* **2001**, *123*, 10705.
- (18) Peterlinz, K. A.; Georgiadis, R. M.; Herne, T. M.; Tarlov, M. J. *J. Am. Chem. Soc.* **1997**, *119*, 3401.
- (19) Schena, M.; Shalon, D.; Davis, R. W.; Brown, P. O. *Science* **1995**, *270*, 467.
- (20) Georgiadis, R.; Peterlinz, K. P.; Peterson, A. W. *J. Am. Chem. Soc.* **2000**, *122*, 3166.
- (21) MacBeath, G.; Schreiber, S. L. *Science* **2000**, *289*, 1760.
- (22) Kane, R. S.; Takayama, S.; Ostuni, E.; Ingber, D. E.; Whitesides, G. M. *Biomaterials* **1999**, *20*, 2363.
- (23) Zhou, H.; Baldini, L.; Hong, J.; Wilson, A. J.; Hamilton, A. D. *J. Am. Chem. Soc.* **2006**, *128*, 2421.
- (24) Fritz, M. C.; Hahner, G.; Spencer, N. D. *Langmuir* **1996**, *12*, 6074.
- (25) Smith, E. A.; Thomas, W. D.; Kiessling, L. L.; Corn, R. M. *J. Am. Chem. Soc.* **2003**, *125*, 6140.
- (26) Hederos, M.; Konradsson, P.; Liedberg, B. *Langmuir* **2005**, *21*, 2971.
- (27) Houseman, B. T.; Mrksich, M. *Chem. Biol.* **2002**, *9*, 443.
- (28) Houseman, B. T.; Gawalt, E. S.; Mrksich, M. *Langmuir* **2003**, *19*, 1522.
- (29) Bryan, M. C.; Plettenburg, O.; Sears, P.; Rabuka, D.; Wacowich-Sgarbi, S.; Wong, C. H. *Chem. Biol.* **2002**, *9*, 713.
- (30) Bryan, M. C.; Wong, C. H. *Tetrahedron Lett.* **2004**, *45*, 3639.
- (31) Fazio, F.; Bryan, M. C.; Blixt, O.; Paulson, J. C.; Wong, C. H. *J. Am. Chem. Soc.* **2002**, *124*, 14397.
- (32) Fazio, F.; Bryan, M. C.; Lee, H. K.; Chang, A.; Wong, C. H. *Tetrahedron Lett.* **2004**, *45*, 2689.
- (33) Fukui, S.; Feizi, T.; Galustian, C.; Lawson, A. M.; Chai, W. *Nat. Biotechnol.* **2002**, *20*, 1011.
- (34) Short, R.; Buttle, D.; Day, A. Sugar Binding Surface. Patent WO2004/04038 A1, 2004.

the gold surface<sup>45</sup>), the dependency of electrostatic attractions upon molecular size<sup>33,34</sup> limiting the range of immobilized carbohydrates,<sup>46</sup> and the substrate-dependent nature of specific covalent attachment chemistries<sup>35–41,43,44</sup> prohibiting application to a wide range of materials and geometries (e.g., the requirement for unique coupling reactions in the case of gold and silicon substrates).

Plasmachemical surface functionalization offers a potential solution to the aforementioned limitations. It ensures covalent bonding to the substrate via free radical sites created at the interface by the electrical discharge during the onset of nanolayer deposition. Furthermore, appropriate choice of precursor containing desired reactive groups in conjunction with a polymerizable carbon–carbon double bond can lead to structurally well-defined functional nanolayers for a whole host of applications (e.g., protein adsorption<sup>47–49</sup>). Typically, electric discharge modulation is employed where a short plasma duty cycle on-time (microseconds) generates active sites in the gas phase as well as at the growing film surface via VUV irradiation, ion and electron bombardment, followed by conventional carbon–carbon double bond polymerization processes proceeding throughout each accompanying extended pulse off-period (milliseconds) in the absence of any UV, ion, or electron-induced damage to the growing film.<sup>50,51</sup> Extremely high levels of surface functionality can be attained by this approach. Examples successfully devised in the past include amine,<sup>52</sup> anhydride,<sup>51</sup> epoxide,<sup>53</sup> carboxylic acid,<sup>54</sup> cyano,<sup>55</sup> halide,<sup>56</sup> hydroxyl,<sup>57</sup> furfuryl,<sup>58</sup> and

**Scheme 1.** Galactosyl Residue Immobilization onto Pulsed Plasma Deposited Poly(allylmercaptan) via Disulfide Bridge Formation



perfluoroalkyl<sup>59</sup> functionalized surfaces. Effectively, any surface that relies on a specific chemistry for its performance can, in principle, be generated by the aforementioned pulsed plasma-chemical methodology.

In this article, we describe two different substrate-independent plasmachemical functionalization methodologies for the fabrication of rewritable carbohydrate microarrays. First, disulfide bridge formation<sup>60</sup> using thiol-reactive glycomethanethiosulfonate (glyco-MTS) reagents<sup>61–63</sup> and thiol-functionalized pulsed plasma deposited poly(allylmercaptan) nanolayers<sup>64</sup> (Scheme 1); the alternative is Schiff base imine formation between the aldehyde terminus present in reducing sugars and surface amine groups<sup>65</sup> presented by pulsed plasma deposited poly(4-vinylaniline) nanolayers (Scheme 2). The deposition of a protective protein-resistant nanolayer over the respective sugar binding layer provides an effective means for preventing nonspecific background protein adsorption (Scheme 3), where the top layer is locally punctured before, or during, microarraying.

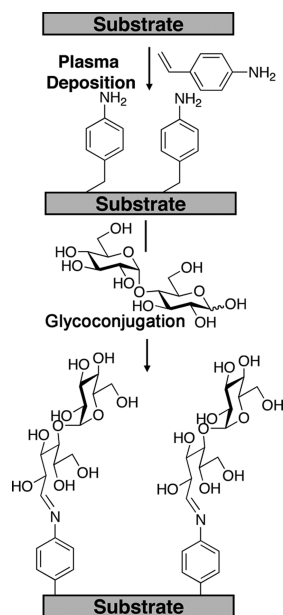
## 2. Experimental Section

**2.1. Plasmachemical Nanolayering.** Plasma polymerization of the respective monomers was carried out in a cylindrical glass reactor (4.5 cm diameter, 460 cm<sup>3</sup> volume) located inside a Faraday cage. This was evacuated by a 30 L min<sup>-1</sup> rotary pump via a liquid

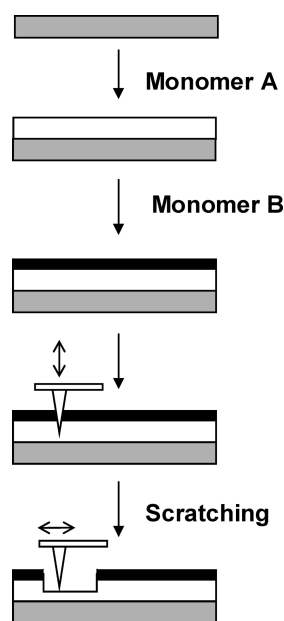
- (35) Stevens, J.; Blixt, O.; Glaser, L.; Taubenberger, P. P.; Paulson, J. C.; Wilson, I. A. *J. Mol. Biol.* **2006**, *355*, 1143.
- (36) Blixt, O.; et al. *Proc. Natl. Acad. Sci. U.S.A.* **2004**, *7*, 17033.
- (37) Zhou, X.; Zhou, J. *Biosens. Bioelectron.* **2006**, *21*, 1451.
- (38) Yates, E. A.; Jones, M. O.; Clarke, C. E.; Powell, A. K.; Simon, R. J.; Porch, A.; Edwards, P. P.; Turnbull, A. K. *J. Mater. Chem.* **2003**, *13*, 2061.
- (39) Schwarz, M.; Spector, L.; Gargir, A.; Avraham, S.; Gortler, M.; Altstock, R. T.; Avinoam, A. D.; Dotan, N. *Glycobiology* **2003**, *13*, 749.
- (40) Adams, E. W.; Ratner, D. M.; Bokesch, H. R.; McMahon, J. B.; O'Keefe, B. R.; Seiberger, P. H. *Chem. Biol.* **2004**, *11*, 876.
- (41) Park, S.; Lee, M. R.; Pyo, S. J.; Shin, I. *J. Am. Chem. Soc.* **2003**, *126*, 4812.
- (42) Park, S.; Shin, I. *Angew. Chem., Int. Ed.* **2002**, *41*, 3180.
- (43) Shirahata, N.; Hozumi, A.; Miura, Y.; Kobayashi, K.; Sakka, Y.; Yonezawa, T. *Thin Solid Films* **2006**, *499*, 213.
- (44) De Smet, L. C. P. M.; Stork, G. A.; Hurenkamp, G. H. F.; Sun, Q. Y.; Huseyin, T.; Vronen, P. J. E.; Sieval, A. B.; Wright, A.; Visser, G. M.; Zuilhof, H.; Sudholter, E. J. R. *J. Am. Chem. Soc.* **2003**, *125*, 13916.
- (45) Flynn, N. T.; Tran, T. N. T.; Cima, M. J.; Langer, R. *Langmuir* **2003**, *19*, 10909.
- (46) Disney, M. D.; Seeberger, P. H. *Drug Discovery Today Targets* **2004**, *3*, 151.
- (47) Zhang, Z.; Menges, B.; Timmons, R. B.; Knoll, W.; Forch, R. *Langmuir* **2003**, *19*, 4765.
- (48) Bullett, N. A.; Whittle, J. D.; Short, R. D.; Douglas, C. W. I. *J. Mater. Chem.* **2003**, *13*, 1546.
- (49) Godek, M. L.; Malkov, G. S.; Fisher, E. R.; Grainger, D. W. *Plasma Processes Polym.* **2006**, *3*, 485.
- (50) Badyal, J. P. S. *Chem. Br.* **2001**, *37*, 45.
- (51) Ryan, M. E.; Hynes, A. M.; Badyal, J. P. S. *Chem. Mater.* **1996**, *8*, 37.
- (52) Oye, G.; Roucoules, V.; Oates, L. J.; Cameron, A. M.; Cameron, N. R.; Steel, P. G.; Davis, B. G.; Coe, D. M.; Cox, R. A.; Badyal, J. P. S. *J. Phys. Chem. B* **2003**, *107*, 3496.
- (53) Tarducci, C.; Kinmond, E.; Brewer, S.; Willis, C.; Badyal, J. P. S. *Chem. Mater.* **2000**, *12*, 1884.
- (54) Hutton, S. J.; Crowther, J. M.; Badyal, J. P. S. *Chem. Mater.* **2000**, *12*, 2282.
- (55) Tarducci, C.; Schofield, W. C. E.; Brewer, S.; Willis, C.; Badyal, J. P. S. *Chem. Mater.* **2001**, *13*, 1800.
- (56) Teare, D. O. H.; Barwick, D. C.; Schofield, W. C. E.; Garrod, R. P.; Ward, L. J.; Badyal, J. P. S. *Langmuir* **2005**, *21*, 11425.

- (57) Tarducci, C.; Schofield, W. C. E.; Brewer, S. A.; Willis, C.; Badyal, J. P. S. *Chem. Mater.* **2002**, *14*, 2541.
- (58) Tarducci, C.; Brewer, S. A.; Willis, C.; Badyal, J. P. S. *Chem. Commun.* **2005**, *3*, 406.
- (59) Coulson, S. R.; Woodward, I. S.; Brewer, S. A.; Willis, C.; Badyal, J. P. S. *Langmuir* **2000**, *16*, 6287.
- (60) Wynn, R.; Richard, F. M. *Methods Enzymol.* **1995**, *251*, 351.
- (61) Davis, B. G.; Maughan, M. A. T.; Green, M. P.; Ullman, A.; Jones, J. B. *Tetrahedron: Asymmetry* **2000**, *11*, 245.
- (62) Matsumoto, K.; Davis, B. G.; Jones, J. B. *Chem. Commun.* **2001**, 903.
- (63) Davis, B. G.; Ward, S. J.; Rendle, P. M. *Chem. Commun.* **2001**, 189.
- (64) Schofield, W. C. E.; McGettrick, J.; Bradley, T. J.; Przyborski, S.; Badyal, J. P. S. *J. Am. Chem. Soc.* **2006**, *128*, 2280.
- (65) Clayden, J.; Greeves, N.; Warren, S.; Wothers, P. *Organic Chemistry*; Oxford University Press: Oxford, 2001.

**Scheme 2.**  $\beta$ -D-Glucosyl Residue Immobilization Using D-Maltose Reacted onto Pulsed Plasma Deposited Poly(4-vinylaniline) via Schiff Base Imine Formation



**Scheme 3.** Molecular Scratchcard Fabrication Followed by SPM Tip Scratching (Where Precursors A and B Are Sugar Reactive and Protein Resistant, Respectively)



nitrogen cold trap ( $2 \times 10^{-3}$  mbar base pressure and better than  $1.2 \times 10^{-9}$  mol  $s^{-1}$  leak rate). A copper coil (4 mm diameter, 10 turns, located 15 cm away from the precursor inlet) was connected to a 13.56 MHz radio frequency power supply via an LC matching network. System pressure was monitored with a Pirani gauge. All fittings were grease free. During pulsed plasma deposition, the RF source was triggered by a signal generator, and the pulse shape was monitored with an oscilloscope. Before each experiment, the apparatus was scrubbed with detergent, rinsed with propan-2-ol, and oven-dried. Further cleaning entailed running a 40 W continuous wave air plasma at 0.2 mbar pressure for 20 min. At this stage, the precursor was loaded into a sealable glass tube and further purified using multiple freeze–pump–thaw cycles. Then the substrate of interest was placed into the center of the reactor, and the system was evacuated to base pressure. For each functional

**Table 1.** Optimum Pulsed Plasma Deposition Parameters Yielding High Structural Retention for Each Functional Precursor

precursor	reactor temp/ $^{\circ}C$	pulse duty cycle/ $\mu s$		deposition rate/nm $min^{-1}$
		time on	time off	
allylmercaptan (+80%, Sigma-Aldrich)	22	100	4000	10
4-vinylaniline (+97%, Sigma-Aldrich)	40	100	4000	20
N-acryloylsarcosine methyl ester monomer (+97%, Lancaster)	50	20	5000	9

**Table 2.** Carbohydrate Solutions Employed in This Study

carbohydrate	concentration
$\beta$ -D-galacto-methanethiosulfonate	1 $\mu M$ in 70 mM CHES buffer (+99%, Sigma-Aldrich)
D-maltose (+90%, Sigma-Aldrich)	1 $\mu M$ in formamide (Sigma-Aldrich)

**Table 3.** Proteins and Their Associated Fluorophores Employed in This Study

protein	fluorophore	label
peanut agglutinin (Molecular Probes)	Alexa Fluor 488	protein I
concanavalin A (Molecular Probes)	Alexa Fluor 647	protein II

monomer, a continuous flow of vapor was introduced via a fine needle control valve at a pressure of 0.2 mbar and  $2.2 \times 10^{-7}$  mol  $s^{-1}$  flow rate for 5 min before electrical discharge ignition. Optimum pulsed plasma duty cycle parameters for each precursor are listed in Table 1. Upon completion of deposition, the RF power source was switched off, and the monomer was allowed to continue purging through the system for a further 5 min before evacuation to base pressure and venting to a nitrogen atmosphere.

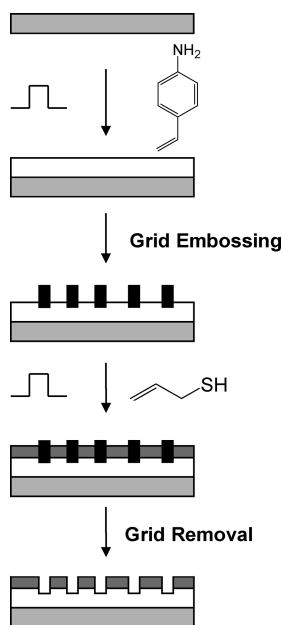
**2.2. Carbohydrate Microarrays.** 2-( $\beta$ -D-Galactopyranosyl)ethyl methanethiosulfonate (Gal-MTS) was synthesized as described previously.<sup>61</sup> Carbohydrate microarrays were fabricated using a robotic microarrayer (Genetix, Inc.) equipped with 1 nL delivery micromachined pins. Carbohydrate  $\beta$ -D-galacto-methanethiosulfonate or D-maltose solutions were spotted onto 300 nm thick pulsed plasma poly(allylmercaptan)- or poly(4-vinylaniline)-coated glass slides ( $18 \times 18 \times 0.17$  mm<sup>3</sup>, BDH) (Table 2). Circular spots with diameters ranging from 100 to 125  $\mu m$  could be routinely obtained. Following spotting, the slides of immobilized carbohydrates were kept in a humidity chamber for 12 h at 32  $^{\circ}C$  and 36 h at 70  $^{\circ}C$ , respectively. The slides were subsequently washed with CHES buffer, CHES buffer diluted to 50% v/v with deionized water, and finally twice with deionized water.

Carbohydrate microarrays were exposed to a complementary solution of protein I (20  $\mu g mL^{-1}$  in phosphate-buffered saline) and protein II (20  $\mu g mL^{-1}$  in phosphate-buffered saline), respectively, for 60 min at room temperature followed by successive rinses in phosphate-buffered saline, phosphate-buffered saline diluted to 50% v/v with deionized water, and twice with deionized water (Table 3).

To demonstrate rewritability, stripping of bound carbohydrates  $\beta$ -D-galacto-methanethiosulfonate and D-maltose from the pulsed plasma deposited nanolayers was investigated by immersing the chips in a boiling solution of 200 nM TrisCl pH 7.0, 0.03 M SSC, and 0.1% (w/v) SDS for 10 min followed by reimmobilization as described in the above protocols.

**2.3. Bifunctional Patterning of Protein Binding Carbohydrates.** Multiplex surface patterning entailed embossing a grid (2000 Mesh, Agar) at 400 MPa for 10 s onto a 300 nm layer of pulsed plasma deposited poly(4-vinylaniline), followed by the pulsed plasma deposition of allylmercaptan (300-nm thickness). Subsequent grid removal produced 10  $\mu m$  poly(allylmercaptan) squares surrounded by 2  $\mu m$  poly(4-vinylaniline) bars (Scheme 4).

**Scheme 4.** Formation of a Patterned Multifunctional Surface via Grid Embossing for Carbohydrate Immobilization



Carbohydrate immobilization onto the bifunctional surface entailed sequential exposure to solutions of Gal-MTS and D-maltose carbohydrates for 12 h at 32 °C and 36 h at 70 °C, respectively. The slides were subsequently washed with CHES buffer, CHES buffer diluted to 50% v/v with deionized water, and twice with deionized water. These bifunctional carbohydrate surfaces were then exposed to a solution containing proteins I and II ( $20 \mu\text{g mL}^{-1}$  per protein in phosphate-buffered saline) for 60 min at room temperature followed by successive rinses in phosphate-buffered saline, phosphate-buffered saline diluted to 50% v/v with deionized water, and twice with deionized water.

**2.4. Carbohydrate Molecular Scratchcards.** Carbohydrate immobilization using the molecular scratchcard approach<sup>66</sup> entailed fabricating a bilayer stack comprising 20 nm pulsed plasma deposited poly(*N*-acryloylsarcosine methyl ester) on top of a 300 nm pulsed plasma deposited carbohydrate linker layer (Scheme 3). The coated slide was then mounted onto an atomic force microscope stage (Digital Instruments Nanoscope III control module, extender electronics, and signal access module). A tapping mode tip (Nanoprobe, spring constant 42–83 N m<sup>-1</sup>) scanning in contact mode was used to scratch away the protein-resistant pulsed plasma poly(*N*-acryloylsarcosine methyl ester) top layer. Tip movement in the *x*, *y*, and *z* planes was controlled by Veeco Nanolithography software (version 5.30r1). The resultant patterned molecular scratchcards were immersed in a solution of Gal-MTS or D-maltose for 12 h at 32 °C or 36 h at 70 °C, respectively, followed by successive rinses in CHES buffer, CHES buffer diluted to 50% v/v with deionized water, and twice with deionized water. These carbohydrate patterned surfaces were then exposed to a solution of protein I ( $20 \mu\text{g mL}^{-1}$  in phosphate-buffered saline) or protein II ( $20 \mu\text{g mL}^{-1}$  in phosphate-buffered saline), respectively, for 60 min at room temperature, followed by successive rinses in phosphate-buffered saline, phosphate-buffered saline diluted to 50% v/v with deionized water, and twice with deionized water.

**2.5. Surface Characterization.** X-ray photoelectron spectroscopy (XPS) was undertaken using a VG ESCALAB MK II surface analysis instrument equipped with an unmonochromated Mg K $\alpha_{1,2}$  X-ray source (1253.6 eV) and a concentric hemispherical analyzer. Photoemitted electrons were collected at a takeoff angle of 30° from the substrate normal, with electron detection in the constant analyzer

energy mode (pass energy = 20 eV). The XPS spectra were charge referenced to the C(1s) peak at 285.0 eV and fitted with a linear background and equal full width at half-maximum Gaussian components<sup>67</sup> using Marquardt minimization computer software. Instrument sensitivity (multiplication) factors derived from chemical standards were taken as being C(1s): S(2p): O(1s): N(1s): equals 1.00: 0.52: 0.63: 0.45.

Fourier transform infrared (FTIR) analysis was carried out using a Perkin-Elmer Spectrum One spectrometer equipped with a liquid nitrogen-cooled MCT detector operating across the 700–4000 cm<sup>-1</sup> range. Reflection–absorption measurements were performed using a variable angle accessory (Specac) set at 66° in conjunction with a KRS-5 polarizer fitted to remove the s-polarized component. All spectra were averaged over 516 scans at a resolution of 1 cm<sup>-1</sup>.

Contact angle analysis was carried out with a video capture system (ASE Products, model VCA2500XE) using 2.0  $\mu\text{L}$  droplets of deionized water.

Film thickness measurements were performed with an nkd-6000 spectrophotometer (Aquila Instruments Ltd.). The obtained transmittance-reflectance curves (over the 350–1000 nm wavelength range) were fitted to the Cauchy model for dielectric materials using a modified Levenberg–Marquardt method.<sup>68</sup>

AFM micrographs were acquired in tapping mode<sup>69</sup> operating in air at room temperature (Digital Instruments Nanoscope III control module, extender electronics, and signal access module).

Fluorescence microscopy was used to demonstrate selective binding of proteins to carbohydrates with an Olympus IX-70 system (DeltaVision RT, Applied Precision). Images were collected using excitation wavelengths of 490 nm (Alexa Fluor 488) and 640 nm (Alexa Fluor 647) to give emissions of 528 nm (FITC) and 685 nm (CY5), respectively.

### 3. Results

**3.1. Carbohydrate Microarrays.** XPS, FTIR, and fluorescence microscopy provided confirmation that disulfide bridge formation (from Gal-MTS) and the Schiff base imine formation (from D-maltose immobilization) had taken place on the respective thiol- and amine-functionalized surfaces.

XPS characterization of the pulsed plasma deposited poly(allylmercaptan) and poly(4-vinylaniline) nanolayers revealed a strong resemblance to the theoretical compositions predicted from the respective monomer structures (Table 4). The absence of any Si(2p) signal from the underlying silicon substrate confirmed that the deposited films were thicker than the XPS sampling depth.

The observed high level of structural retention was confirmed by infrared spectroscopy. Allylmercaptan precursor displays stretching absorbances corresponding to allyl C–H (3080 cm<sup>-1</sup>), allyl CH<sub>2</sub> (3031 cm<sup>-1</sup>), alkyl CH<sub>2</sub> (2891 cm<sup>-1</sup>), thiol S–H (2555 cm<sup>-1</sup>), and allyl C=C (1634 cm<sup>-1</sup>)<sup>64</sup> (Figure 1). All of these features are clearly discernible following pulsed plasma deposition, except for the allyl carbon–carbon double bond stretches, which disappear as a consequence of polymerization. Exposure to Gal-MTS gave rise to an attenuation of the thiol S–H stretch (2555 cm<sup>-1</sup>) and the appearance of OH stretching (3300 cm<sup>-1</sup>), which is indicative of disulfide formation between the carbohydrate and functional nanolayer.

Characteristic infrared bands for the 4-vinylaniline monomer were as follows:<sup>70</sup> asymmetric amine stretch (3440 cm<sup>-1</sup>), symmetric amine stretch (3350 cm<sup>-1</sup>), aromatic CH stretch

(67) Evans, J. F.; Gibson, J. H.; Moulder, J. F.; Hammond, J. S.; Goretzki, H. *Fresenius' J. Anal. Chem.* **1984**, 319, 841.

(68) Tabet, M. F.; McGahan, W. A. *Thin Solid Films* **2000**, 370, 122.

(69) Zhong, Q.; Innis, D.; Kjoller, K.; Ellings, V. B. *Surf. Sci.* **1993**, 14, 3045.

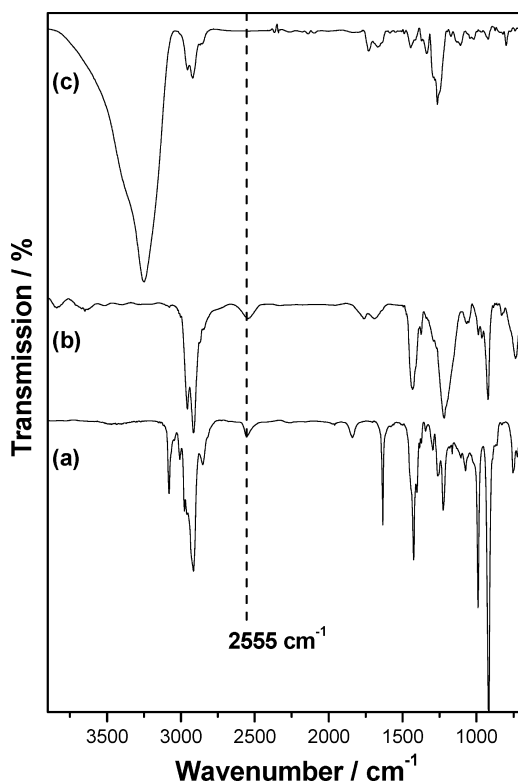
(66) Harris, L. G.; Schofield, W. C. E.; Badyal, J. P. S. *Chem. Mater.* **2007**, 19, 1546.

**Table 4.** XPS Elemental Compositions and Water Sessile Drop Contact Angle Values for Pulsed Plasma Deposited Poly(allylmercaptan), Poly(4-vinylaniline), Poly(*N*-acryloylsarcosine Methyl Ester), and Poly(*N*-acryloylsarcosine Methyl Ester) Deposited on Top of Poly(allylmercaptan) or Poly(4-vinylaniline)

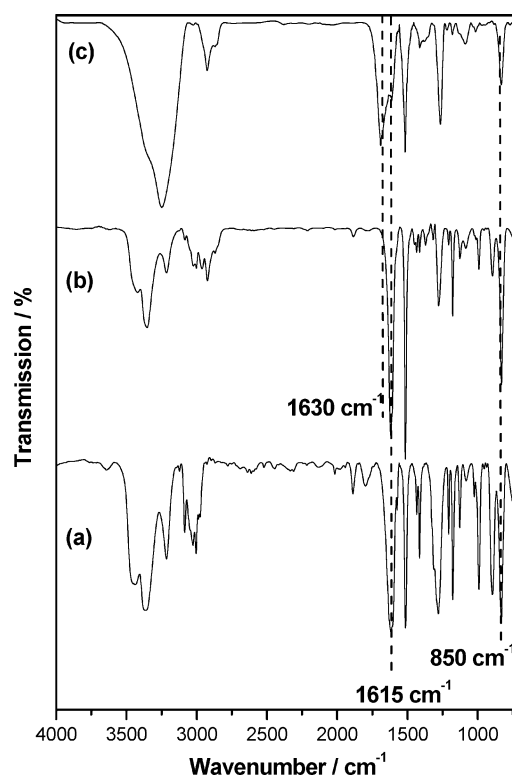
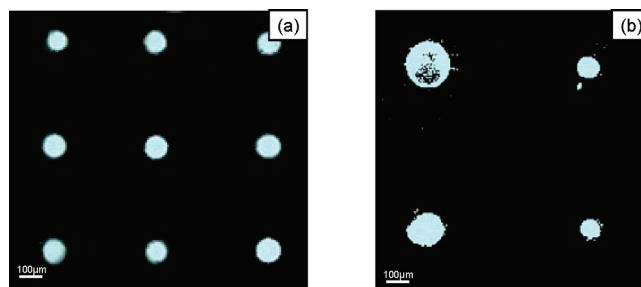
pulsed plasma nanolayer(s)	contact angle/deg	XPS elemental composition			
		C %	N %	O %	S %
allylmercaptan	82 ± 1	74 ± 1			27 ± 1
theoretical allylmercaptan	N/A	75	0	0	25
4-vinylaniline	71 ± 2	88 ± 1	12 ± 1		
theoretical 4-vinylaniline	N/A	89	11		
<i>N</i> -acryloylsarcosine methyl ester	52 ± 3	64 ± 2	10 ± 1	27 ± 1	
theoretical <i>N</i> -acryloylsarcosine methyl ester	N/A	64	9	27	
<i>N</i> -acryloylsarcosine methyl ester/allylmercaptan	53 ± 2	64 ± 1	10 ± 1	26 ± 1	
<i>N</i> -acryloylsarcosine methyl ester/4-vinylaniline	53 ± 3	65 ± 1	10 ± 1	26 ± 1	

(3090  $\text{cm}^{-1}$ ), ring summation (1880  $\text{cm}^{-1}$ ), C=C stretch (1625  $\text{cm}^{-1}$ ),  $\text{NH}_2$  deformations (1615  $\text{cm}^{-1}$ ), para-substituted aromatic ring stretch (1500  $\text{cm}^{-1}$ ),  $=\text{CH}_2$  deformations (1415  $\text{cm}^{-1}$ ), aromatic C–N stretch (1300  $\text{cm}^{-1}$ ), para-substituted benzene ring stretch (1170  $\text{cm}^{-1}$ ), HC=CH trans wag (990  $\text{cm}^{-1}$ ),  $=\text{CH}_2$  wag (910  $\text{cm}^{-1}$ ), and  $\text{NH}_2$  wag (850  $\text{cm}^{-1}$ ) (Figure 2). All of these absorbances were retained following pulsed plasma deposition, except for the vinyl carbon–carbon double bond features, which underwent polymerization. Subsequent exposure to D-maltose gave rise to an attenuation of the amine  $\text{NH}_2$  wag (850  $\text{cm}^{-1}$ ) and  $\text{NH}_2$  deformation (1615  $\text{cm}^{-1}$ ) intensities, accompanied by the appearance of OH (3250  $\text{cm}^{-1}$ ) and C=N (1630  $\text{cm}^{-1}$ ) stretches, which are all indicative of Schiff base imine formation between the carbohydrate and surface amine groups.

The carbohydrate chemistry used here allowed the use of Gal-MTS reagent to create  $\beta$ -D-galactosyl-displaying arrays and use of D-maltose to create  $\alpha$ -D-glucosyl-displaying arrays. Retention

**Figure 1.** Infrared spectra of (a) allylmercaptan monomer, (b) pulsed plasma deposited poly(allylmercaptan), and (c)  $\beta$ -D-galactosyl residues immobilized onto poly(allylmercaptan) via disulfide bond formation using reagent Gal-MTS.

of biological activity following surface immobilization of the respective carbohydrates was verified by fluorescence microscopy. Selective binding of fluorescent proteins I and II was observed for the respective microarrays of  $\beta$ -D-galactosyl and  $\alpha$ -D-glucosyl residues (Figure 3). The selective binding of

**Figure 2.** Infrared spectra of (a) 4-vinylaniline monomer, (b) pulsed plasma deposited poly(4-vinylaniline), and (c) D-maltose immobilized onto poly(4-vinylaniline).**Figure 3.** Fluorescence image of (a)  $\beta$ -D-galactosyl array on poly(allylmercaptan) following exposure to complementary fluorescent protein I (PNA) and (b)  $\alpha$ -D-glucosyl array on poly(4-vinylaniline) after exposure to complementary fluorescent protein II (ConA).

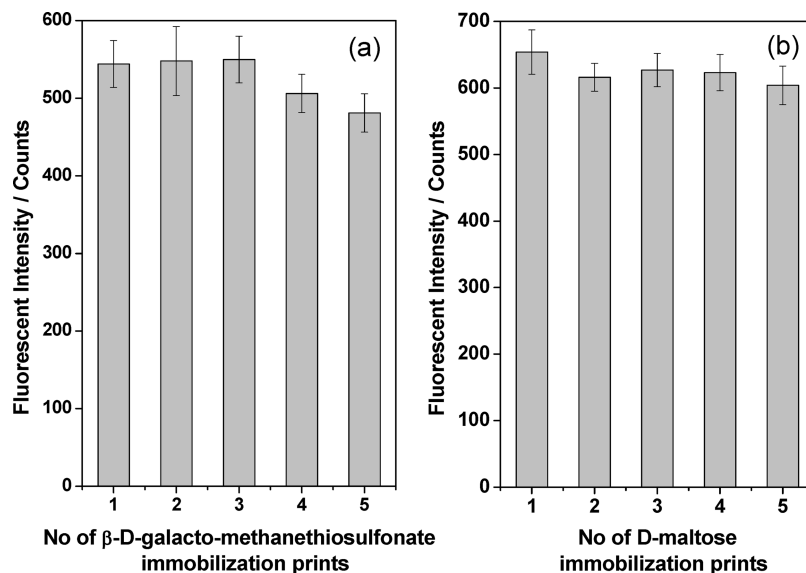


**Figure 4.** Fluorescence intensity following stripping and reimmobilization of (a)  $\beta$ -D-galactosyl on poly(allylmercaptan) and then exposure to protein I and (b) D-maltose on poly(4-vinylaniline) and then exposure to protein II. (The fluorescence signal dropped to the background level for each fully stripped/denatured sample in between rewriting of the respective carbohydrate.)

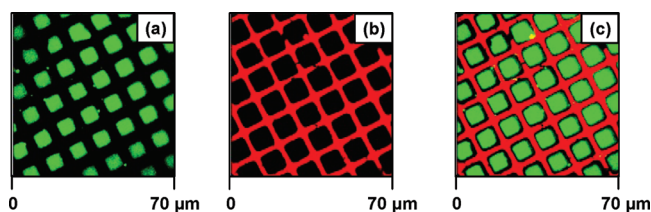


**Figure 5.** Fluorescence microscopy for  $\beta$ -D-galactosyl functionalized poly(allylmercaptan) squares and  $\alpha$ -D-glucosyl-functionalized poly(4-vinylaniline) bars following exposure to (a) protein I, (b) protein II, and (c) a mixture of proteins I and II.

Protein I PNA to the  $\beta$ -D-galactosyl array and of Protein II ConA to the  $\alpha$ -D-glucosyl array is entirely consistent with the previously determined ligand preferences of these lectins.

The rewritability of these functionalized slides was demonstrated by using high-stringency washes to strip the immobilized carbohydrates from the surface, followed by repeat carbohydrate immobilization and then exposure to the complementary protein. It was found that the fluorescence intensity remained approximately constant as a function of the number of times the surface-bound carbohydrates were stripped and reattached for both  $\beta$ -D-galacto-methanethiosulfonate and D-maltose microarrays (Figure 4).

**3.2. Bifunctional Patterning of Protein Binding Carbohydrates.** Pulsed plasma deposition of poly(4-vinylaniline) onto a substrate, followed by embossing a grid and then poly(allylmercaptan) coating gave rise to a bifunctional surface amenable to the region-specific immobilization of carbohydrates (Scheme 4). Retention of biological activity was demonstrated by immersion in a mixed solution of proteins I and II. Binding of protein I was found to occur only to regions of  $\beta$ -D-galactosyl-functionalized poly(allylmercaptan), while protein II binding targeted areas of  $\alpha$ -D-glucosyl displayed on poly(4-vinylaniline) (Figure 5). The highly specific nature of carbohydrate–protein binding is evident from the absence of cross-

contamination of the respective fluorescent proteins between areas of alternating carbohydrate functionalization.

**3.3. Carbohydrate Molecular Scratchcards.** The viability of plasmachemical nanolayering for the fabrication of a molecular scratchcard entailed the pulsed plasma deposition of either poly(allylmercaptan) ( $\beta$ -D-galacto-methanethiosulfonate reactive layer) or poly(4-vinylaniline) (D-maltose reactive layer), followed by the overcoating of a 20 nm thick protein-resistant poly(*N*-acryloylsarcosine methyl ester) film (Scheme 3). The absence of cross-contamination during pulsed plasma deposition was verified by the measured XPS elemental composition and contact angle values for each bilayer stack matching those of poly(*N*-acryloylsarcosine methyl ester) (Table 4).

Subsequent rastering of an SPM tip to scratch  $1\ \mu\text{m} \times 1\ \mu\text{m}$  squares in the protein-resistant overlayer exposed the underlying reactive functionalities (Figure 6). Subsequent exposure to Gal-MTS and then protein I demonstrated the reactivity of the

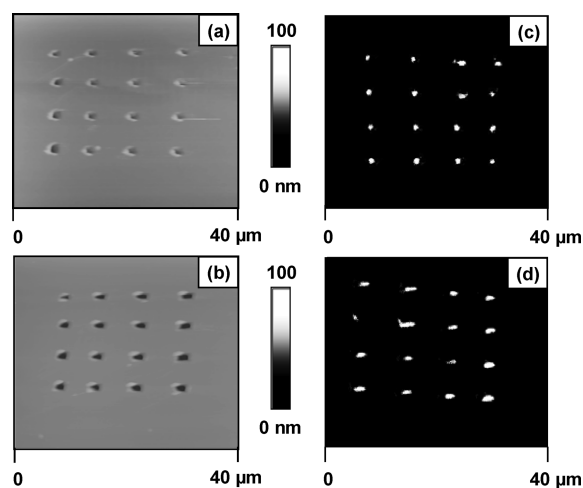


**Figure 6.** AFM micrographs of a  $4 \times 4$  array of exposed reactive pixels surrounded by a protein-resistant background: (a) thiol functionalities and (b) amine functionalities. The corresponding fluorescence images following: (c) reaction of Gal-MTS with (a) and then exposure to protein I, and (d) immobilization of D-maltose to display  $\alpha$ -D-glucosyl onto (b) and then exposure to protein II.

(70) Lin-Vein, D.; Colthup, N. B.; Fateley, W. G.; Grasselli, J. G. *The Handbook of Characteristic Frequencies of Organic Molecules*; Academic Press: London, 1991.

exposed thiol pixels, while sequential exposure to D-maltose and protein II confirmed the reactivity of the exposed amine pixels.

#### 4. Discussion

The structural diversity of carbohydrates allows them to participate in a plethora of important biological processes.<sup>71,72</sup> Hence, glycomic arrays are becoming recognized as a powerful tool for understanding and optimizing complex biological systems. The prerequisites are that they need to be robust and reproducible and carbohydrate biological activity is maintained. Numerous approaches have been developed for this purpose but are known to either be restricted to a limited range of carbohydrates<sup>33,34</sup> or suffer from nontransferable substrate surface chemistries.<sup>35–41,43,44</sup> The described pulsed plasma-chemical functionalization approach provides substrate-independent scaffolds for the immobilization of carbohydrates as well as the elimination of nonspecific background protein adsorption via the molecular scratchcard concept. Viability was demonstrated by depositing poly(allylmercaptan) films, which readily undergo disulfide bridge formation with appropriate carbohydrate methanethiosulfonate (MTS) reagents and poly(4-vinylaniline) layers amenable to Schiff base imine formation with the aldehyde terminus of reducing sugars. Biological activity of these immobilized carbohydrates was exemplified by binding fluorescently labeled galactose-specific lectin protein peanut agglutinin<sup>73,74</sup> (protein I) and maltose-specific lectin protein concanavalin A<sup>75,76</sup> (protein II), respectively (Table 3 and Figure 3). The regeneration/rewritability of the functional surfaces was confirmed by stripping the carbohydrate microarrays and then rewriting the carbohydrates/proteins without measuring any significant loss of immobilization/binding efficiencies. This unique attribute can be explained in terms of the deposited layers having a gel-like structure.<sup>77</sup>

Specific carbohydrate–protein binding interactions were exemplified by the use of sequential depositions of poly(allylmercaptan) and poly(4-vinylaniline) in conjunction with a mask to create a bifunctional surface comprising 10  $\mu\text{m}$  poly(allylmercaptan) squares separated by 2  $\mu\text{m}$  poly(4-vinylaniline) bars. These bifunctional surfaces were found to display specific carbohydrate immobilization, which in turn led to their respective carbohydrate biological selectivities.

Finally, it was shown that plasmachemical nanolayering can be used to create functional stacks, for instance, with a protein-resistant top layer to eliminate nonspecific protein adsorption.<sup>78</sup> Bilayer stacks comprising 20 nm protein-resistant poly(*N*-acryloylsarcosine methyl ester) on top of poly(allylmercaptan) or poly(4-vinylaniline) underlayers were fabricated. Subsequent removal of the protein-resistant top layer using an SPM tip to expose underlying reactive thiol or amine groups, followed by reaction with Gal-MTS or D-maltose, respectively, demonstrates retention of biological activity by observing the binding of fluorescent proteins I (PNA) and II (ConA), respectively. Therefore, in principle, multiple carbohydrate probes for proteins can be patterned simultaneously or consecutively onto a surface using a simple robotic liquid-delivering system, in the absence of cross-contamination between different probes. An array-manufacturing process based upon such surface chemistries could easily be automated and scaled up.

#### 5. Conclusions

Thiol- and amine-functionalized pulsed plasma deposited nanolayers can be utilized for the immobilization of carbohydrates amenable to specific protein binding. These thiol- and amine-functionalized nanolayers have been found to be highly stable toward stripping and rewriting of carbohydrate arrays. The sequential deposition of a reactive nanolayer and then a passivation nanolayer can be used in conjunction with localized mechanical piercing of the passive top layer to expose underlying reactive groups for preparing carbohydrate arrays surrounded by a protein-resistant background.

**Supporting Information Available:** Complete ref 36. This material is available free of charge via the Internet at <http://pubs.acs.org>.

JA901294R

(71) Kim, J. H.; Yanh, H.; Park, J.; Boons, G. J. *J. Am. Chem. Soc.* **2005**, *127*, 12090.

(72) Nagahori, N.; Nishimura, S. I. *Biomacromolecules* **2001**, *2*, 22.

(73) Gunther, G. R.; Wang, J. L.; Yahara, I.; Cunningham, B. A.; Edelman, G. M. *Proc. Natl. Acad. Sci. U.S.A.* **1973**, *70*, 1012.

(74) Mandal, D. K.; Brewer, C. F. *Biochemistry* **1993**, *31*, 5116.

(75) Lotan, R.; Skutelsky, E.; Danon, D.; Sharon, N. *J. Biol. Chem.* **1975**, *250*, 8518.

(76) Liener, I. E.; Sharon, N.; Goldstein, I. J. *The Lectins*; Academic Press: New York, 1986.

(77) Tarducci, C.; Schofield, W. C. E.; Brewer, S.; Willis, C.; Badyal, J. P. S. *Macromolecules* **2002**, *35*, 8724.

(78) Vroman, L.; Adams, A. L.; Fischer, G. C.; Munoz, P. C. *Blood* **1980**, *55*, 156.